Supplementary Information

Supplementary Materials and Methods

Materials. Pathologist-dissected breast tumor, patient-matched peripheral normal breast tissue, and normal cervical tissue samples were obtained from anonymous donors through the Pathology Biorepository and Research Core of the University of Maryland Greenebaum Cancer Center. Rabbit anti-TTP antibodies were from Abcam, as were horseradish peroxidase-conjugated mouse anti-β-actin and rabbit anti-GAPDH antibodies. Mouse anti-FLAG M2 monoclonal and all secondary antibodies were from Sigma. DNA oligonucleotide primers for RT-PCR and quantitative real-time RT-PCR (qRT-PCR) assays were from Integrated DNA Technologies, and are as follows:

amplification of ARE-BP 3'-coding and 3'UTR fragments for probing cDNA arrays

AUF1-f1	5'- GAACCAGTGAAGAAGATAATGG -3'
AUF1-r1	5'- GACTTGCTCTACAATACTGGG -3'
TIA-1-f1	5'- CCAGTATATGCCTAATGGTTGG -3'
TIA-1-r1	5'- CAGGAATGCAAACTAGAACTGC -3'
TTP-f1	5'- CGACTCCCCATCTTCAATCG -3'
TTP-r1	5'- CAAGGGAAGCAGACGACCC -3'
HuR-f1	5'- GTCTGAATGAGAAGTGAGAAGG -3'
HuR-r1	5'- GCAATGTGTGGACAGAAACTCG -3'

amplification of cDNA encoding TTP open reading frame

TTP-f2	5'- GCTCCTCGAGATGGATCTGACTGCCATCTACG -3' (XhoI site underlined)
TTP-r2	5'- GCACGAATTCTGTCACTCAGAAACAGAGATGC -3' (EcoRI site underlined)

generation of TTP C147R mutant (sense strand only shown)

TTPmut	5'- CCAAATACAAGACGGAACTCCGTCACAAGTTCTACCTCC -3' (mutated base underlined)

qRT-PCR primer sets

human VEGF SYBR primer set #1
hVEGF-f1 5'- AAATGCTTTCTCCGCTCTGA -3'
hVEGF-r1 5'- CCCACTGAGGAGTCCAACAT -3'

human VEGF SYBR primer set #2
hVEGF-f2 5'- GGGCAGAATCATCACGAAGT -3'
hVEGF-r2 5'- ATCTGCATGGTGATGTTGGA -3'

human GAPDH SYBR primer set
hGAPDH-f1 5'- TGCACCACCAACTGCTTAGC -3'
hGAPDH-r1 5'- GGCATGGACTGTGGTCATGAG -3'

human VEGF Taqman primer set
hVEGF-f3 5'- GCACCCATGGCAGAAGG -3'
hVEGF-r3 5'- CTCGATTGGATCGCAGTAGCT-3'
hVEGF-Tq 5'- 56-FAM/CTGATACACATCCATCAACTTCACCACTTCGT/3BHQ_1/ -3'

human GAPDH Taqman primer set
hGAPDH-f2 5'- GACAGTCAGCCGCATCTTC -3'
hGAPDH-r2 5'- ACTCCGACCTTCACCTTCC -3'
hGAPDH-Tq 5'- 5TEX613-Y/CGCCAGCCGAGCCACATCGC/3BHQ_2/ -3'

murine VEGF SYBR primer set
mVEGF-f1 5'- CACGACAGAAGGAGAGCAGAAG -3'
mVEGF-r1 5'- CTCAATCGGACGGCAGTAGC -3'

murine GAPDH SYBR primer set
mGAPDH-f1 5'- ATGGTGAAGGTCGGTGTGAACG -3'
mGAPDH-r1 5'- CGCTCCTGGAAGATGGTGATGG -3'

cDNA probes for Cancer Profiling Array. cDNA probes (500 – 700 nucleotides) encoding the 3' end of the coding sequence and proximal 3'UTR of AUF1, TTP, HuR, and TIA-1 mRNAs were amplified from hepatoblastoma HepG2 cell total RNA using the Access RT-PCR kit (Promega) and gene specific primer sets (above). BLAST homology searches (1) against the RefSeq database (http://www.ncbi.nlm.nih.gov/RefSeq) indicated that these fragments share no significant homology with any other known human mRNAs. Purified cDNA fragments were radiolabeled using [^{32}P-α]dATP (6000 Ci/mmol; Perkin Elmer) with the Prime-it II Random Primer Labeling Kit (Stratagene) as directed by the manufacturer and purified using Quick Spin G-50 DNA Purification columns (Roche).

Recombinant DNA materials. A cDNA encoding the complete open reading frame of human TTP was amplified by RT-PCR using total RNA from human THP-1 mononuclear cells and oligonucleotide primers TTP-f2 and TTP-r2, and then subcloned into pGEM-T-Easy (Promega). A single base mutation converting Cys147→Arg (C147R) was introduced by site-directed mutagenesis using the QuikChange II XL kit (Stratagene) programmed with mutagenic primer TTP-mut and its reverse complement. Wild type and C147R mutant TTP cDNAs were then inserted into plasmid pTRE2hyg (Clontech) downstream of a cDNA fragment encoding three in-frame copies of the FLAG epitope excised from plasmid p3XFLAG-CMV-10 (Sigma) using standard subcloning techniques, yielding plasmids pT2hyg-FLAG-TTPwt and pT2hyg-FLAG-TTP C147R, respectively. The fidelity of all recombinant DNA materials was verified by automated DNA sequencing.

Tissue/cell lysis and Western blot analyses. Lysates were prepared for parallel RNA/protein purification from human tissues using the RNeasy Mini kit (Qiagen), with proteins isolated by acetone precipitation as directed by the manufacturer and clarified by centrifugation at 12,000 x *g* for 10 min. HeLa and MEF cell lysates were prepared by washing cell monolayers with phosphate buffered saline followed by scraping in 2 x SDS-PAGE buffer (250 mM Tris [pH 6.8] containing 2% SDS, 10% glycerol, and 0.05% bromophenol blue). Lysates were incubated at 100 °C for 5 min, then clarified by centrifugation at 12,000 x *g* for 10 min. Protein extracts were fractionated through 10% SDS-polyacrylamide gels, transferred to Immobilon membranes (Millipore) and blocked in 5% milk in PBS with 5% non-fat milk in Tris buffered saline containing 0.1% Tween-20 for 1 h at room temperature. Blocked membranes were incubated overnight at 4 °C with primary antibodies as indicated and washed. Following 1 h incubations with peroxidase-conjugated secondary antibodies, immunoblots were washed and developed using Super Signal West Pico Chemiluminescent detection method (Pierce).

Measurement of VEGF mRNA levels. Total RNA was purified from HeLa lines or MEFs using TRIzol reagent (Invitrogen) according to the manufacturer's instructions. For HeLa cell RNA, steady-state VEGF mRNA levels were measured by multiplex, qRT-PCR using the iScript One-Step RT-PCR Kit for Probes (Bio-Rad) with human VEGF and GAPDH Taqman primer sets. All DNA primers are listed above. For RNA purified from MEFs, VEGF mRNA levels were determined using the SuperScript III Platinum SYBR Green One-Step qRT-PCR kit (Invitrogen) with murine VEGF and GAPDH SYBR primer sets in parallel reactions. In both cases, relative VEGF mRNA concentrations were calculated by comparison of threshold cycle numbers (C_t) to standard curves and normalized to endogenous GAPDH mRNA levels. Each data point was taken as the mean ± standard deviation from triplicate qRT-PCR reactions for each RNA sample.

Immunoprecipitation and RT-PCR of ribonucleoprotein complexes. HeLa cells were lysed for 10 min on ice in PLB buffer (10 mM HEPES [pH 7.5] containing 100 mM KCl, 5 mM $MgCl_2$, 0.3% Nonidet P-40, 1 mM DTT, 100 U/ml RNase inhibitor and protease inhibitors). The lysates were incubated (2 h, 4 °C) with 100 µl of a 50% (v/v) suspension of Protein-A Sepharose beads (Sigma) precoated with 30 µg each of control mouse IgG_1 (BD Pharmingen) or M2 anti-Flag monoclonal antibody. The beads were washed five times with NT2 buffer (50 mM Tris [pH 7.4] containing 150 mM NaCl, 1 mM $MgCl_2$, 0.05% Triton X-100). For RNA analysis, the beads were incubated with 100 µl NT2 buffer containing RNase-free DNase I (20 U) for 15 min at 30 °C, washed twice with 1 ml NT2 buffer, and further incubated in 100 µl NT2 buffer containing 0.1% SDS and 0.5 mg/ml proteinase K for 15 min at 55 °C to digest the proteins bound to the beads. RNA was purified by extraction with phenol:chloroform, and then reverse-transcribed using random hexamers and SuperScript II reverse transcriptase (Invitrogen). Specific cDNAs were then quantified by real-time PCR using the Power SYBR Green PCR Master Mix (Applied

Biosystems) with human VEGF SYBR primer sets #1 and #2, and the human GAPDH SYBR primer set (above).

Supplementary Figure Legends

Supplementary Figure S1. Distribution plots of TTP mRNA levels from additional gene array datasets were constructed using the Oncomine v3 utility as described in Fig. 2. The number of patient samples analyzed (*n*) is indicated for each tissue pool. Analysis methods, statistical comparisons, and dataset sources are included in Supplementary Table S2. Literature citations correspond to references contained within this Supplementary Information file.

Supplementary Figure S2. Poly (ADP-ribose) polymerase (PARP) cleavage verifies that staurosporine-induced HeLa cell death is apoptotic. Staurosporine (100 nM) was added to cultures of untransfected and FLAG-TTP-expressing HeLa cells. At indicated time points, whole cell lysates were prepared as described under "Supplementary Materials and Methods". To prevent losing cells that had lifted from tissue flask surfaces due to cell death, the medium was carefully removed and centrifuged for 5 min at 300 × *g*, with recovered material incorporated into the lysate. Protein extracts were fractionated by SDS-PAGE and analyzed for PARP cleavage by Western blot. Bands corresponding to full length PARP (116 kDa) and the large caspase-3 cleavage product of PARP (89 kDa) are indicated.

Supplementary Figure S3. Influence of TTP on tumorigenic phenotypes in a non-transformed cell model. (*A*) Western blot showing TTP and GAPDH protein levels in MEFs from TTP knockout mice (-/-) and wild-type littermates (+/+). The minor band remaining in extracts from the $TTP^{-/-}$ MEFs likely represents a cross-reactive protein target, possibly a TTP family member.

(*B*) Proliferation assays of $TTP^{-/-}$ and $TTP^{+/+}$ MEFs performed as described in Fig. 3. (*C*) The sensitivity of $TTP^{-/-}$ (*closed circles*) and $TTP^{+/+}$ (*open circles*) MEFs to pro-apoptotic stimuli staurosporine (*left*) and cisplatin (*right*) were assessed as described in Fig. 3. IC_{50} values from replicate independent experiments were resolved as described under "Materials and Methods", and are listed in Supplementary Table S4. (*D*) Relative VEGF mRNA levels and (*E*) VEGF mRNA turnover rates in $TTP^{-/-}$ and $TTP^{+/+}$ MEFs were measured as described in Fig. 4. Parameters describing VEGF mRNA decay kinetics in MEF models are given in the text.

Supplementary Figure S4. VEGF mRNA levels do not correlate with TTP expression in prostate cancer. Relative TTP and VEGF mRNA levels were extracted from an array dataset (GEO Acc# GSE6919; described in Ref. 2) containing gene expression profiles for 89 primary (*black circles*) and metastatic (*green circles*) human prostate tumors. Correlation analysis of VEGF versus TTP mRNA levels demonstrated no relationship between these transcripts (r = -0.038; P = 0.72). Dotted lines indicate the 95% confidence intervals of the regression solution.

Supplementary Table S1: cDNA array analyses of differential ARE-BP expression in between tumor and peripheral non-transformed tissues[a]

ARE-BP	$\log_2$(T/N) < -1[b]	$\log_2$(T/N) > 1[c]
AUF1	20 (13%)	20 (13%)
TIA-1	35 (22%)	41 (27%)
TTP	100 (65%)	7 (5%)
HuR	22 (14%)	18 (12%)

[a]values based on ratio of ^{32}P-labeled cDNA probe hybridization to cDNA prepared from paired tumor (T) and non-transformed peripheral (N) tissues on a Cancer Profiling II Array (BD Biosciences) representing 154 patients.

[b]number (and %) of tumor samples displaying a 50% decrease in ARE-BP mRNA levels relative to paired normal tissue

[c]number (and %) of tumor samples displaying a 100% increase in ARE-BP mRNA levels relative to paired normal tissue

Supplementary Table S2: DNA microarray analyses showing repression of TTP mRNA in cancer[a]

Tissue	Class 1 (*n*)	Class 2 (*n*)	Median 1[b]	Median 2[b]	*P* value[c]	GEO acc #[d]	Ref.[e]
lung	normal (17)	squamous cell carcinoma (21)	2.0660	1.2112	4.5×10^{-6}	not deposited	(3)
lung	normal (11)	adenocarcinoma (11)	2.5223	1.5584	1.1×10^{-4}	not deposited	(4)
lung	normal (19)	adenocarcinoma (20)	2.2452	1.6327	6.3×10^{-6}	GSE2514	(5)
ovary	normal (4)	adenocarcinoma (28)	2.0759	0.7722	1.8×10^{-6}	not deposited	(6)
cervix	normal (8)	carcinoma (20)	2.9463	2.3710	4.3×10^{-4}	GSE6791	(7)
liver	normal (76)	carcinoma (104)	2.2875	1.6263	7.1×10^{-11}	GSE3500	(8)
bone marrow	normal (22)	smoldering multiple myeloma (12)	1.7443	2.3804	8.0×10^{-6}	GSE5900	(9)
prostate	carcinoma (64)	metastatic cancer (25)	2.0256	1.2912	3.8×10^{-14}	GSE6919	(2)
prostate	carcinoma (59)	metastatic cancer (20)	2.1428	-2.0876	1.9×10^{-13}	not deposited	(10)
prostate	carcinoma (23)	metastatic cancer (9)	2.5882	1.1538	2.0×10^{-6}	not deposited	(11)

[a]studies selected from the Oncomine database (www.oncomine.org) filtered for differential TTP mRNA expression with $P < 0.001$.

[b]signal intensity for each array spot is expressed on a $\log_2$ scale. Intensity values from individual arrays are then normalized by setting the median signal to 0 and the standard deviation to 1. Quoted values are the median normalized expression levels for TTP across *n* independently analyzed samples. Distribution plots are in Fig. 2C and Supplementary Fig. S1.

[c]statistical significance between TTP expression in each tissue class assessed by the Oncomine utility using the unpaired *t* test.

[d]GEO database accession numbers (www.ncbi.nlm.nih.gov/geo) for deposited datasets.

[e]published studies describing the generation of individual array datasets.

Supplementary Table S3: Comparison of TTP expression in normal versus cancerous tissues by EST and SAGE frequency

Database[a]	Tissue Source	TTP frequency		*P versus* normal[b]
		raw	%	
EST	normal	266 / 3362444	0.0079%	
	cancer	115 / 2519339	0.0046%	< 0.01
SAGE	normal	4780 / 68609428	0.0070%	
	cancer	2521 / 69075786	0.0036%	< 0.01

[a]Expression of TTP was compared between normal and cancerous tissues across all tissue types based on the recovery frequency of TTP-encoding Expressed Sequence Tags (ESTs) and Serial Analysis of Gene Expression (SAGE) tags by querying the Cancer Genome Anatomy Project (CGAP) database (http://cgap.nci.nih.gov) using sequence ID NM_003407.

[b]The CGAP database computes the sequence odds ratio as:

$$\frac{\text{Seqs A / Total Sequences in A}}{\text{Seqs B / Total Sequences in B}}$$

The significance of differences in transcript expression is then calculated using a Bayesian analysis approach described in Ref. 12.

Supplementary Table S4: Influence of TTP on cellular sensitivity to pro-apoptotic stimuli

cell line	TTP status[a]	apoptotic stimulus	IC_{50}[b]	*n*
HeLa	basal	staurosporine	45 ± 7 nM	3
	wt overexpressed	staurosporine	19 ± 5 nM	4
	C147R overexpressed	staurosporine	61 ± 8 nM	4
HeLa	basal	cisplatin	13 ± 1 μM	4
	wt overexpressed	cisplatin	16 ± 3 μM	4
	C147R overexpressed	cisplatin	14 ± 2 μM	4
MEF	-/-	staurosporine	54 ± 6 nM	3
	+/+	staurosporine	>1000 nM	4
MEF	-/-	cisplatin	>50 μM	2
	+/+	cisplatin	>50 μM	2

[a]TTP levels manipulated by stable ectopic overexpression or chromosomal knockout as described in Fig. 3 and Supplementary Fig. S3.

[b]The concentration of each drug yielding 50% cell death in 24 hours (IC_{50}) was calculated from dose-response experiments as described in Fig. 3. Each value represents the mean ± SD for *n* independent experiments. The extreme resistance of MEF $TTP^{-/-}$ cells to cisplatin-induced cell death or $TTP^{+/+}$ cells to either apoptotic stimulus precluded accurate estimation of IC_{50} values in these cases.

Supplementary Table S5: Candidate TTP substrate mRNAs encoding pro-oncogenic products

mRNA	Genbank Accession #	Putative TTP binding sites		Notes	Refs
		sequence[a]	location[b]		
AKT1	NM_005163	uaauuuauu (8/9)	+1648	Ser/Thr kinase that suppresses apoptosis by phosphorylating and inactivating components of the apoptotic machinery	(13)
BCL2	NM_000633	uuauuuauu (9/9) uuauuuaug (8/9)	+973 +3193	outer mitochondrial membrane protein – inhibits apoptosis in some cell types including lymphocytes	(14)
CCND1	M73554	auauuuauu (8/9) uuauuauu (8/9) uuauuauu (8/9)	+2310 +3380 +3389	cyclin D1 - overexpression alters cell cycle progression in a variety of tumors	(15)
CDK2	NM_001798	uuauuauu (8/9) uauuuau (7/7)	+1234 +1821	essential for cell cycle G1/S phase transition directing cell proliferation	(16)
CYR61	NM_001554	uuauuuauc (8/9) uuauuuaug (8/9)	+1673 +1767	cysteine-rich angiogenic inducer 61 - increased expression is associated with an aggressive breast cancer cell phenotype	(17)
DP-1	NM_007111	uuauuuagu (8/9)	+1452	cell cycle-regulating transcription factor - may have a role in hepatocellular carcinoma progression by promoting tumor cell growth	(18)
FBN2	NM_001999	uuauuuauu (9/9)	+9128	fibrillin-2 - component of microfibrils that contributes to migration of lung fibroblasts	(19)
PLAUR	NM_002659	uuauuauu (8/9) uuauuuauu (9/9)	+1225 +1279	urokinase plasminogen activator receptor - promotes cell motility and metastasis	(20)
VEGF	NM_001025366	uuauuuaau (8/9) uauuuau (7/7) uuauuuauu (9/9) uauuuau (7/7)	+2470 +2568 +2973 +3075	increases vascular permeability to induce angiogenesis, also promotes cell migration and inhibits apoptosis	(21)

[a]Putative TTP-binding sequences were identified based on the following criteria:

(i) Sequence must be located downstream of the termination codon in each mRNA (ie: in the 3'UTR)

(ii) Consensus TTP target sequences of UUAUUUAUU were permitted a single substitution or deletion (although both A residues must be present)

(iii) Abbreviated TTP target sequences of UAUUUAU were permitted no variations

Sequence determinants for high affinity TTP binding were described in Ref. 22.

[b]The location of each putative TTP-binding motif is indicated relative to the translational initiation codon.

Supplementary References

1. Johnson M, Zaretskaya I, Raytselis Y, Merezhuk Y, McGinnis S, Madden TL. NCBI BLAST: a better web interface. Nucleic Acids Res 2008;36:W5-W9.

2. Yu YP, Landsittel D, Jing L, et al. Gene expression alterations in prostate cancer predicting tumor aggression and preceding development of malignancy. J Clin Oncol 2004;22:2790-2799.

3. Bhattacharjee A, Richards WG, Staunton J, et al. Classification of human lung carcinomas by mRNA expression profiling reveals distinct adenocarcinoma subclasses. Proc Natl Acad Sci USA 2001;98:13790-13795.

4. Powell CA, Spira A, Derti A, et al. Gene expression in lung adenocarcinomas of smokers and nonsmokers. Am J Respir Cell Mol Biol 2003;29:157-162.

5. Stearman RS, Dwyer-Nield L, Zerbe L, et al. Analysis of orthologous gene expression between human pulmonary adenocarcinoma and a carcinogen-induced murine model. Am J Pathol 2005;167:1763-1775.

6. Welsh JB, Zarrinkar PP, Sapinoso LM, et al. Analysis of gene expression profiles in normal and neoplastic ovarian tissue samples identifies candidate molecular markers of epithelial ovarian cancer. Proc Natl Acad Sci USA 2001;98:1176-1181.

7. Pyeon D, Newton MA, Lambert PF, et al. Fundamental differences in cell cycle deregulation in human papillomavirus-positive and human papillomavirus-negative head/neck and cervical cancers. Cancer Res 2007;67:4605-4619.

8. Chen X, Cheung ST, So S, et al. Gene expression patterns in human liver cancers. Mol Biol Cell 2002;13:1929-1939.

9. Zhan F, Barlogie B, Arzoumanian V, et al. Gene-expression signature of benign monoclonal gammopathy evident in multiple myeloma is linked to good prognosis. Blood 2007;109:1692-1700.

10. Dhanasekaran SM, Barrette TR, Ghosh D, et al. Delineation of prognostic biomarkers in prostate cancer. Nature 2001;412:822-826.

11. LaTulippe E, Satagopan J, Smith A, et al. Comprehensive gene expression analysis of prostate cancer reveals distinct transcriptional programs associated with metastatic disease. Cancer Res 2002;62:4499-4506.

12. Strausberg RL, Buetow KH, Emmert-Buck MR, Klausner RD. The Cancer Genome Anatomy Project: building an annotated gene index. Trends Genet. 2000;16:103-106.

13. Gong J, Lee J, Akio H, Schlegel PN, Shen R. Attenuation of apoptosis by chromogranin A-induced Akt and survivin pathways in prostate cancer cells. Endocrinology 2007;148:4489-4499.

14. Park J, Choi Y, Suh S, et al. Bcl-2 overexpression attenuates resveratrol-induced apoptosis in U937 cells by inhibition of caspase-3 activity. Carcinogenesis 2001;22:1633-1639.

15. Wang Y, Thakur A, Sun Y, et al. Synergistic effect of cyclin D1 and c-Myc leads to more aggressive and invasive mammary tumors in severe combined immunodeficient mice. Cancer Res 2007;67:3698-3707.

16. Du J, Widlund HR, Horstmann MA, et al. Critical role of CDK2 for melanoma growth linked to its melanocyte-specific transcriptional regulation by MITF. Cancer Cell 2004;6:565-576.

17. Lin M, Chang C, Chen S, et al. Cyr61 expression confers resistance to apoptosis in breast cancer MCF-7 cells by a mechanism of NF-κB-dependent XIAP up-regulation. J Biol Chem 2004;279:24015-24023.

18. Yasui K, Arii S, Zhao C, et al. *TFDP1*, *CUL4A*, and *CDC16* identified as targets for amplification at 13q34 in hepatocellular carcinomas. Hepatology 2002;35:1476-1484.

19. McGowan SE, Holmes AJ, Mecham RP, Ritty TM. Arg-Gly-Asp-containing domains of fibrillins-1 and -2 distinctly regulate lung fibroblast migration. Am J Respir Cell Mol Biol 2008;38:435-445.

20. Thomas S, Chiriva-Internati M, Shah GV. Calcitonin receptor-stimulated migration of prostate cancer cells is mediated by urokinase receptor-integrin signaling. Clin Exp Metastasis 2007;24:3635-37719.

21. Carmeliet P. VEGF as a key mediator of angiogenesis in cancer. Oncology 2005;69 Suppl. 3:4-10.

22. Brewer BY, Malicka J, Blackshear PJ, Wilson GM. RNA sequence elements required for high affinity binding by the zinc finger domain of tristetraprolin: Conformational changes coupled to the bipartite nature of AU-rich mRNA-destabilizing motifs. J Biol Chem 2004;279:27870-27877.

Supplementary Figure S1

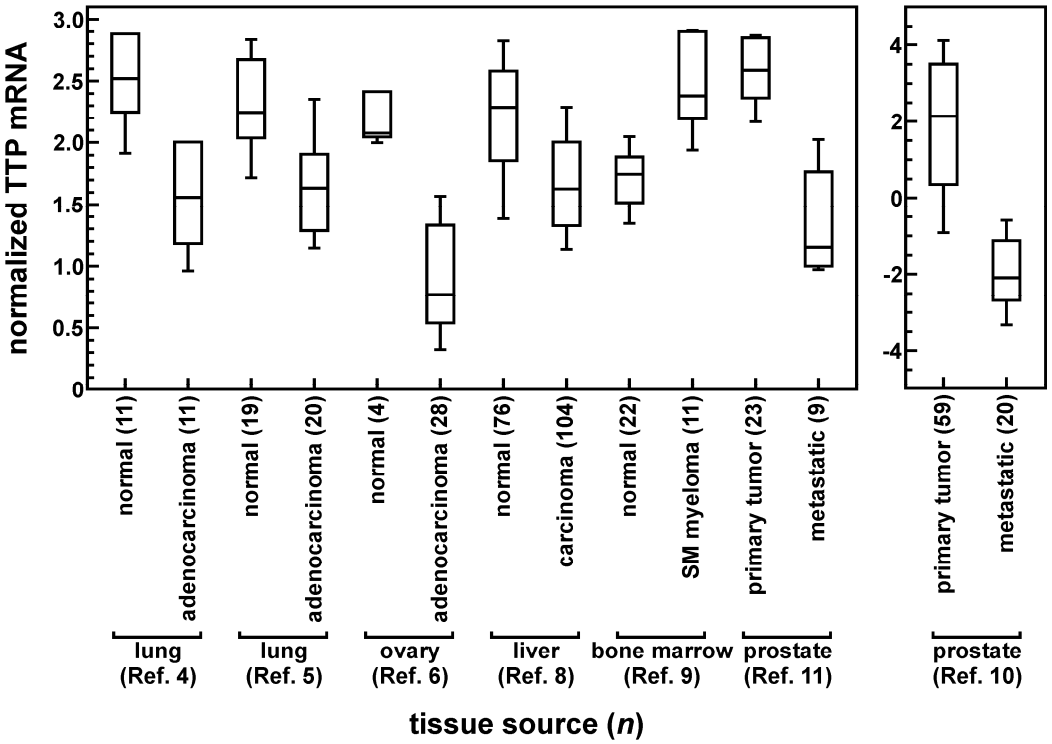

Supplementary Figure S2

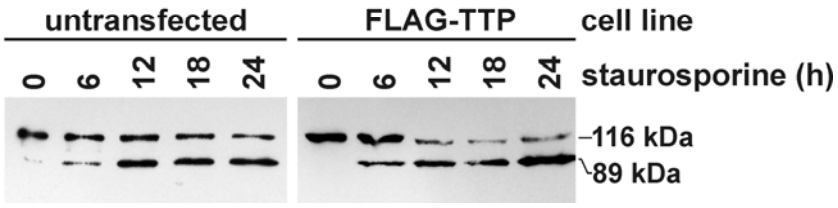

Supplementary Figure S3

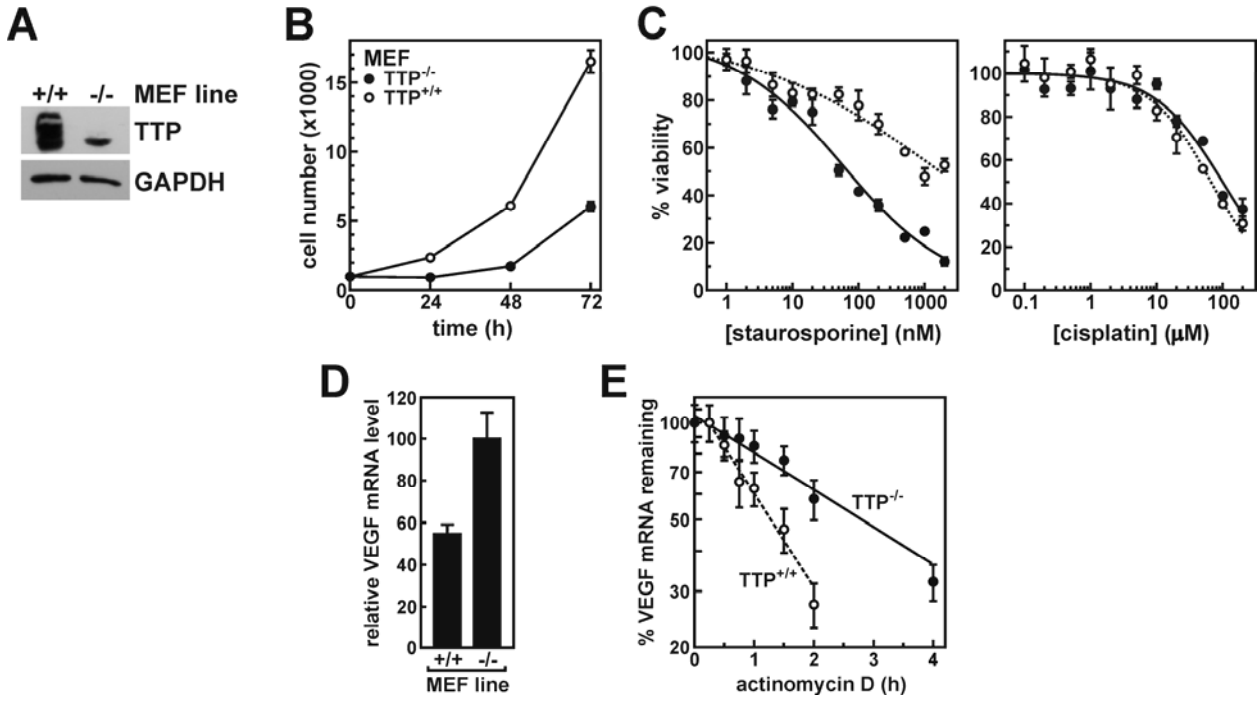

Supplementary Figure S4